USP7 Inhibition Induces Apoptosis in Glioblastoma by Stabilizing ARF4

Tingzheng Pan
First Affiliated Hospital of Soochow University
Xuetao Li
First Affiliated Hospital of Soochow University
Zhennan Tao
First Affiliated Hospital of Soochow University
Hui Yao
First Affiliated Hospital of Soochow University
Yue Wu
First Affiliated Hospital of Soochow University
Guangliang Chen
First Affiliated Hospital of Soochow University
Kai Zhang
First Affiliated Hospital of Soochow University
Youxin Zhou (brain_lab@suda.edu.cn)
First Affiliated Hospital of Soochow University https://orcid.org/0000-0002-2835-8376
Yulun Huang
First Affiliated Hospital of Soochow University

Primary research

Keywords: GBM, USP7, Ubiquitination, ARF4, Apoptosis

Posted Date: June 1st, 2021

DOI: https://doi.org/10.21203/rs.3.rs-552140/v1

Abstract

Background: Glioblastomas (GBMs) are grade IV central nervous system tumors characterized by a poor prognosis and a median overall survival of 15 months. The glioblastoma cell population is more genetically unstable, resistant to chemotherapy, more angiogenic, and more malignant. Because ubiquitin-specific proteases (USPs) remove ubiquitin from oncogenic protein substrates, effective inhibition of ubiquitin-specific protease 7 (USP7), which is highly expressed in GBMs, is a potentially critical therapeutic approach.

Methods: Immunohistochemistry and Western blotting were used to detect high expression of USP7 in GBM. in vitro studies were performed by Western blotting, immunofluorescence, and flow cytometry to detect apoptosis following inhibition of USP7. Anti-apoptotic substrates of USP7 were defined by Co-IP and TMT proteomics. Nude mouse intracranial xenograft models were constructed to verify whether inhibition of USP7 inhibited the proliferation rate of tumours.

Results: USP7 is significantly upregulated in glioblastoma samples. Interfering with USP7 in GBMs induced significant apoptosis, which also occurred after treatment with P5091, a novel small molecule inhibitor of USP7. Mechanistically, apoptosis of GBMs after interference with USP7 function is achieved by stabilizing a key anti-apoptotic protein, ADP-ribosylation factor 4 (ARF4).Furthermore, USP7 interacts directly with ARF4 and catalyzes the removal of the K48-linked polyubiquitinated chain that binds to ARF4, thereby stabilizing the protein. In in vivo experiments, P5091 significantly inhibited tumor growth and promoted the expression of apoptotic genes.

Conclusion: Targeted inhibition of USP7 enhances the ubiquitination of ARF4 and ultimately mediates the apoptosis of GBM cells. In a clinical sense, P5091 as a specific inhibitor of USP7 may be an effective approach for the treatment of GBM.

Background

Glioblastomas (GBMs) are grade IV central nervous system tumors characterized by a poor prognosis [1] and a median overall survival that remained at around 15 months for decades. [2] Comprehensive treatments for glioblastoma, such as maximal surgical resection, chemotherapy, and radiation therapy, do not benefit all patients equally and their adverse effects can seriously affect quality of life.[3, 4] Therefore, individualized treatment targeting several abnormal epigenetic functions in GBM should be considered as a potentially valuable approach for these patients.

Ubiquitination is a post-translational modification in which ubiquitin (Ub) molecules are sequentially bound to lysine residues of substrate proteins by Ub-activating enzyme E1, Ub-binding enzyme E2, and Ub-ligase E3.[5] Regulated by the ubiquitin-proteasome system (UPS), ubiquitinated proteins are degraded by the proteasome. [6] UPS regulates the degradation of most proteins in the cell, thus determining various biological functions and playing an important role in many processes.[7] Deubiquitinating enzymes (DUBs) rescue the degradation of substrate proteins by cleaving polyubiquitin and

monoubiquitin to extend the half-life of the target protein.[8] Ubiquitin-specific proteases (USPs), with more than 60 members, are the largest subfamily of deubiquitinating enzymes. A member of the USP family, ubiquitin-specific protease 7 (USP7; also known as Herpesvirus-associated ubiquitin-specific protease, HAUSP) is a cysteine protease originally identified as a binding partner for the herpes simplex viral (HSV) protein infected cell protein 0 (ICP0/Vmw110). [9] USP7 was first thought to deubiquitinate the tumor suppressor gene p53, [10] but Ub-ligase MDM2 is now known to regulate the stability of p53 together with USP7. [11] Numerous proteins are potential substrates for USP7, such as phosphatase and tensin homologue deleted in chromosome 10 (PTEN), [12] forkhead box protein O4 (FOXO4), [13]thyroid hormone receptor-interacting protein 12 (TRIP12),[14]and N-Myc.[15] Many specific substrates of USP7 are oncogenic factors, and they play a key role in the epigenetic control of tumor proliferation, migration, and angiogenesis.

ADP-ribosylation factors (ARFs) are 20 kDa small guanine nucleotide-binding proteins belonging to the Ras superfamily of small G proteins, originally identified as proteins that stimulate the ADP-ribosyltransferase activity of cholera toxin in vitro.[16] ARFs function in a variety of cellular processes, including vesicle transport, cell division, and tumor invasion, and are activators of phospholipase D (PLD). [17] There are three classes of ARF family members: class I (ARF1, -2, and − 3), class II (ARF4 and − 5), and class III (ARF6). Class I and class III ARFs are involved in the transport of intracellular plasma membrane systems,[18]but relatively little is known about the function of class II ARF proteins.[16] ARF4 induces apoptosis in tumors by reducing reactive oxygen species (ROS) production in response to BAX or N-(4-hydroxy-phenyl) retinamide, and thus ARF4 is a tumor anti-apoptotic protein.[19, 20] However, the molecular mechanism underlying the stability of ARF4 in glioma cells, especially in GBM cells, is unclear.

Here, we evaluated the effect of targeted inhibition of USP7-induced apoptosis in GBM cells. Our results show that targeted inhibition of USP7 may be a promising therapeutic strategy for the treatment of GBM.

Materials And Methods

Patients, cell lines, and cultures

Human GBM tissue samples and normal brain contusion tissues were obtained from the First Affiliated Hospital of Soochow University, Suzhou, China. This study was approved by the Ethics Committee of Soochow University. Human SHG-140 cell lines were obtained from the Department of Neurosurgery & Brain and Nerve Research Laboratory, The First Affiliated Hospital of Soochow University, Suzhou, China, after primary culture and identification by STR. T98G cell lines were obtained from the Cell Bank of the Chinese Academy of Sciences (Shanghai, China). Cells were cultured in DMEM (Gibco, USA) containing 10% fetal bovine serum (FBS).

Antibodies

Anti-USP7 (CST#4833; western blotting, 1:1000; immunoprecipitation, 1:50), anti-BAX (CST#89477; western blotting, 1:1000), anti-CLEAVED-CASPASE 3 (CST#9664; western blotting, 1:1000;

immunofluorescence, 1:500), anti-β-tubulin (CST#2146; western blotting, 1:1000), and anti-Ub (CST#3933; western blotting, 1:1000) were purchased from CST, USA. Anti-Bcl-2 (Ab692; western blotting, 1:1000; immunofluorescence, 1:500), anti-ARF4 (Ab171746; western blotting, 1:1000; immunoprecipitation, 1:50), anti-K48 linkage-specific Ub (ab140601; western blotting, 1:1000), and anti-K63 linkage-specific Ub (ab179434; western blotting, 1:1000) were obtained from Abcam (UK). Horseradish peroxidase-labeled goat anti-mouse IgG and goat anti-rabbit IgG (immunofluorescence, 1:1000) were purchased from ZSGB-Bio (China). P5091 (s7132), CHX (s7418), and MG132 (s2619) were purchased from Selleck (USA).

Lentiviral transfection

GeneChem (China) designed two shRNAs against USP7, shUSP7-1: 5’ -UGUAUCUAUUGACUGCCCUTT- 3 ’ and shUSP7-2: 5’ -UGGAUUUGUGGUUACGUUACUC- 3’, and a non-silencing control. Lipofectamine 3000 was used for co-transfection for 8 h, and transfection efficiency was investigated after transfection. Lentiviral shRNA targeting the USP7 gene was generated using the GV112 vector (hU6-MCS-CMV-Puromycin; GeneChem, China). ARF4 overexpression lentivirus was prepared using the GV692 vector (Ubi-MCS- 3FLAG-CBh-gcGFP-IRES-Puromycin; GeneChem). The constructed lentiviral vector was transfected into cells followed by puromycin intervention, and the transfection efficiency was identified by western blotting analysis to screen for stably transfected cell lines.

Immunohistochemistry

Tissues were paraffin-embedded and sectioned for immunostaining. Slides were dewaxed in xylene, then rehydrated in graded ethanol, followed by quenching of endogenous peroxidase activity with 0.3% hydrogen peroxide (China), and strong antigen recovery solution was heated to 37 ◦C to recover the antigen. Non-specific proteins were blocked with 5% goat serum (Solarbio, China). Primary antibodies (1:100 dilution) were used to incubate the sections overnight at 4 ◦C, followed by addition of appropriate biotinylated secondary antibodies (1:100 dilution) (ZSGBBio, China) for 60 min at 37 ◦C. Next, slides were incubated with ABC peroxidase and diaminobenzidine (ZSGBBio) and then counterstained with Mayer's hematoxylin solution (Solarbio) for nuclear staining. For HE staining, slides were deparaffinized and rehydrated. Slides were re-stained by nuclear staining and subsequently using the HE kit (Solarbio). Images were acquired using an inverted microscope (Olympus, Japan).

Western blotting and immunofluorescence analyses

After induction, cells were collected in lysis buffer, incubated on ice for 30 min, and centrifuged at 12 000 × *g* at 4°C for 10 min. The supernatant was collected and the protein concentration determined. Equal amounts of protein samples were subjected to 8–12% SDS-PAGE, transferred to PVDF membranes, and incubated at room temperature or 1 h using 5% skim milk with primary antibody overnight. Membranes were washed with PBST buffer for 30 min and then incubated with a secondary antibody for exposure. For immunofluorescence, cells induced on slides were fixed with 4% paraformaldehyde and permeabilized with 0.5% Triton for 15 min. Slides were incubated at room temperature with 5% BSA for 1 h, BSA was discarded, and mouse anti-BCL2 antibody and rabbit anti-CLEAVED-CASPASE3 antibody were

added for overnight incubation. The next day, the primary antibody was discarded and the secondary antibody was incubated with Alexa Fluor 594-labeled goat anti-rabbit (1:200) and Alexa Fluor 488-labeled goat anti-mouse (1:200) for 1 h at 37°C in a light-proof oven at a constant temperature. Fluorescence microscopy and image acquisition were performed under light-proof conditions.

Cell viability assay (CCK-8 assay)

P5091 were added to 96-well plates containing cell suspensions in a total volume of 100 μl. After induction for 24, 48, and 72 h, 10 μl of CCK8 reagent (Dojindo, Japan) was added and incubated at 37°C for 2 h in a constant temperature incubator. Cell viability was evaluated by measuring the difference in optical density values at 450 nm using an enzymatic standard.

Annexin V-FITC/PI flow cytometry for apoptosis detection

After apoptosis induction, cells were digested with 0.25% trypsin and centrifuged at 2 000 × *g* for 3 min at 4°C, resuspended in pre-chilled PBS, and centrifuged again at 2 000 × *g* for 3 min at 4°C. The supernatant was discarded and the cell precipitate was added to Annexin V-FITC, PI, and binding buffer (BD, USA). After incubation for 10 min at 4°C protected from light, cell fluorescence was detected by flow cytometry.

Tandem mass tags proteomics analysis

Tandem mass tag (TMT) proteomic analysis was performed as follows. Total protein was extracted for concentration determination by SDS-PAGE, trypsin digestion, and TMT peptide labeling. Equal amounts of labeled samples were mixed and separated by chromatography. Samples were loaded onto a pre-column Acclaim PepMap100 100 μm × 2 cm (RP-C18, Thermo Fisher) at a flow rate of 300 nl/min, and then separated on an analytical column (Acclaim PepMap RSLC, 75 μm × 15 cm; RP-C18, Thermo Fisher). Finally, samples were analyzed by LC-MS/MS with primary MS mass resolution set to 60 000, automatic gain control to 3e6, and maximum injection time to 50 ms. Mass spectrometry scan was set to full scan charge to mass ratio m/z range 350–1500, and the scan was performed for the 20 highest peaks. MS/MS spectra were acquired using data-dependent positive ion, the MS/MS resolution was set to 15000, the automatic gain control to 2e5, the maximum ion accumulation time to 40 ms, and the dynamic exclusion time to 30 s.

Immunoprecipitation (IP) and mass spectrometry

Cells were washed twice with pre-cooled PBS and lysed with cell lysis buffer supplemented with protease inhibitors. After removal of insoluble material by centrifugation at 12 000 × *g*, pre-lysates were incubated with protein A/G magnetic beads overnight at 4°C. Precipitates were washed three times with lysis buffer, boiled in 1 x SDS sample buffer for 5 min, and proteins resolved by SDS-PAGE on 8 %–12% gels. Immunoblot detection was performed using appropriate antibodies. For MS, immunoprecipitation was performed as described above, and immunoprecipitates were resolved on SDS-PAGE denaturing gels, stained with Coomassie Blue, and then analyzed by MS. MS was performed with a Q-Exactive mass spectrometer (Thermo Scientific). Parent ion scan range was 350–2000 m/z, mass spectrometry was scanned in data-dependent acquisition, and the most intense 20 fragmentation profiles were acquired

after each full scan (MS2 scan) by high-energy collision dissociation (HCD), NCE energy at 28, and dynamic exclusion time at 25 s.MS1 resolution at M/Z 200 was 70 000, AGC target was set to 3e6, maximum injection time to 100 ms, MS2 resolution to 17 500, AGC target to 1e5, and maximum injection time to 50 ms.

Nude mouse intracranial xenograft model

Female BALB/c nude mice (4–5 weeks, 15–17 g) were purchased from the Animal Center of the Institute of Oncology, Chinese Academy of Medical Sciences (Beijing, China). A total of 5 × 104 SHG-140 cells with luciferase-encoding lentivirus (GeneChem, Shanghai, China) were stereotactically injected into mice (six per group). The lentiviral vectors were GV260 and Ubi-MCS-Luc-IRES-puromycin. P5091 was dissolved in 20% DMSO, 40% PEG-300, and 40% PBS. Seven days after implantation, mice were injected intraperitoneally with equal doses of 10 mg/kg/day, 5 mg/kg/day of P5091, or PBS 2 days per week during the survival period. Intracranial tumor size was assessed and radiance values recorded on days 7, 14, and 28 using the IVIS Spectral Real-Time Imaging System (Blandford, USA). Live mouse brains were removed, fixed in 4% paraformaldehyde, embedded in paraffin, and subjected to HE and IHC. Animal studies were performed according to internationally accepted norms and national regulations.

Statistical analysis

Statistical analyses were performed with SPSS 16.0 or GraphPad Prism 8.2.1 software. Bar statistical plots were expressed by the mean standard deviation of at least three times the number of experimental replicates. Differences between two groups were assessed by Student's t-test, and differences between multiple groups were tested by one-way analysis of variance (ANOVA) followed by Tukey's post hoc test. Bars are expressed as mean ± s.d. or mean ± s.e.m. Statistical significance is shown at #P = NS, *P < 0.05,**P < 0.01,***P < 0.001, or ****P < .0001.

Ressults

USP7 is highly expressed in GBM cells and its inhibition induces apoptosis

Because USP7 is associated with patient prognosis and disease progression in gliomas,[21] we focused on the effects of targeted inhibition of USP7 in GBM. Immunohistochemical (IHC) analysis of tissue sections shows that USP7 expression was significantly higher in GBM than in normal brain tissue (Fig. 1A). We observed similar results using protein extracts from tissues of GBM patients and normal brain (Fig. 1B). Together, these results indicate that USP7 is highly expressed in GBM cells, which we used as a basis for targeting USP7 for GBM treatment. To more accurately study the effect of interference with USP7 function on the behavior of GBM cells and to make the study results more clinically relevant, we used the GBM cell line SHG-140 established by primary culture from human adult male glioblastoma that is highly tumorigenic. [22]

Next, we focused on the biological significance of USP7 interference. Inhibition of USP7 induces apoptosis in neuroblastoma,[23], breast cancer[24] and ovarian cancer cells.[25] We used two different interfering RNAs to transfect SHG-140 and T98G cells and western blot analysis to examine USP7 expression. The results show that USP7 expression significantly decreased (Fig. 1C, 1D). The expression of apoptosis-related proteins was also examined after transfection. As shown in Fig. 1C, 1D, the expression of BCL2 was decreased and the expression of BAX and CLEAVED-CASPASE 3 was significantly increased in SHG-140 and T98G cells transfected with shRNAs compared with the control, indicating that these cells underwent significant apoptosis. Under the same treatment, we determined the expression of apoptosis-related proteins by immunofluorescence and obtained consistent results (Fig. 1E). To investigate changes in apoptosis rate after transfection of SHG-140 and T98G cells with shRNAs, we used Annexin V-FITC/PI flow cytometry. The results show that the apoptosis rates of both types of cells were significantly increased after transfection with shRNAs (Fig. 1F). Together, the above results demonstrate that USP7 is highly expressed in GBM cells, and inhibition of USP7 function with interfering RNA significantly induces apoptosis.

The USP7 inhibitor P5091 induces apoptosis in GBM cells

P5091 is a novel and potent covalent inhibitor of USP7 with selective deubiquitination activity (EC50 = 4.2 ± 0.9 mM) compared to other inhibitors.[26] We evaluated the effect of P5091 on the viability of SHG-140 and T98G cells using the Cell Counting Kit-8. Treatment with different concentrations of P5091 for different times resulted in a significant decrease in the viability of both cell lines (Fig. 2A). The toxic effects of P5091 on SHG-140 and T98G cells were time- and concentration-dependent, and we chose the optimal treatment time of 48 h. The IC50 of SHG-140 and T98G cells were 1.2 μM and 1.59 μM, respectively, when treated with P5091 for 48 h. Based on IC50, SHG-140 and T98G cells were treated with P5091 for 48 h at 1, 2, and 4 μM. To explore whether P5091 induced apoptosis in GBM cells, we used Annexin V-FITC/PI flow cytometry. The results show that the apoptosis rate of SHG-140 and T98G cells increased significantly with increasing treatment concentrations compared to the control group (Fig. 2B). Similarly, we performed western blotting analysis to examine the levels of apoptosis-related proteins in SHG-140 and T98G cells treated with different concentrations of P5091 for 48 h. As shown in Figs. 2C, 2D, there were no significant changes in BCL2, BAX, and CLEAVED-CASPASE 3 after treatment with 1 μM P5091 for 48 h compared with the DMSO control. After treatment with 2 μM and 4 μM P5091 for 48 h, BCL2 protein expression was significantly reduced, and BAX and CLEAVED-CASPASE 3 protein expression was significantly increased in a concentration-dependent manner. These results are consistent with those of immunofluorescence (Fig. 2E). The above results indicate that P5091 has a significant pro-apoptotic effect on GBM cells, and the apoptotic effect increases with increasing concentration.

ARF4 binds to USP7 and is downregulated by USP7 inhibition

To determine the mechanism by which USP7 affects apoptosis in GBM cells, we used a combination of Co-IP and LC-MS/MS to identify USP7-binding proteins in SHG-140 cells. Using this approach, 217

proteins were identified as USP7-binding proteins. We then subjected the identified proteins to KEGG pathway analysis, and Fig. 3A and 3B show the top 10 and top 20 KEGG pathways in terms of significance, which are highly correlated with proteasome function. Protein interaction analysis between the identified proteins and KEGG pathways revealed that the proteasome pathway was highly significant, as shown in Fig. 3C. We then treated SHG-140 cells with DMSO and P5091 (2 μM, 48 h) and subjected the final protein extracts to TMT proteomic analysis. We found changes in the content of 368 proteins, including an increase in 227 proteins and a decrease in 141 proteins. A heat map (Fig. 3D) shows the expression of these differentially expressed proteins. Finally, we pooled and analyzed the 217 proteins identified by Co-IP with the differentially expressed protein results from proteomics, and found that 10 proteins overlapped, including ARF4 (Fig. 3E). These proteins may be direct substrates of USP7 and their expression was altered by P5091 treatment. Here, we focused on ARF4 in view of its association with the anti-apoptotic effects of tumor cells. A volcano plot in Fig. 3F shows the downregulation of ARF4 expression in proteomic detection, and Fig. 3G shows the secondary mass spectra of the four peptides of ARF4. We then performed a correlation analysis between USP7 and ARF4 using the TCGA database, and Fig. 3H shows a significant correlation between these two genes. In summary, we screened for ARF4, a protein that binds to and is affected by USP7 repression, and hypothesized that USP7 affects ARF4 through the proteasome pathway..

Overexpression of ARF4 rescues apoptosis resulting from USP7 interference

First, we attempted to verify the relationship between USP7 and ARF4 proteins in SHG-140. In Co-IP experiments, we found that USP7 and ARF4 bind to each other in a complex (Fig. 4A). In addition, inhibition of USP7 expression in SHG-140 cells using P5091 and shRNA was followed by a decrease in ARF4 protein (Fig. 4B, 4C), which is consistent with our previous analysis. To further determine whether ARF4 is associated with apoptosis in GBM cells, we assessed the effect of ARF4 overexpression in SHG-140 and T98G cells on apoptosis in cells with shRNA inhibition of USP7 or after induction with P5091. First, we assessed the changes in apoptosis rate by Annexin V-FITC/PI flow cytometry (Fig. 4D, 4E). ARF4 overexpression effectively prevented apoptosis induced by USP7 inhibition using shRNA or P5091. We then used western blotting to detect the changes in apoptosis-related proteins. As shown in Fig. 4F-4I, after ARF4 overexpression in cells under both induction conditions, no significant difference in apoptosis-related proteins was observed compared with the blank control group, and apoptosis-related proteins were significantly back-regulated compared with the intervention group. Together, these results suggest that ARF4 has an anti-apoptotic effect on GBM cells and that overexpression of ARF4 counteracts apoptosis induced by targeting USP7

USP7 regulates ARF4 stability through K48-linked deubiquitination

USP7 regulates the stability of substrate proteins through its deubiquitinating enzyme properties. Therefore, we further investigated the relationship between USP7 and the stability of ARF4. We found that interference of USP7 with P5091 or shRNA led to a decrease in the half-life of ARF4 after induction of different treatment groups at 0 h, 5 h, 10 h, and 15 h using CHX (100 μg/ml) (Fig. 5A, 5B). In addition, treatment with the proteasome inhibitor MG132 (10 μM, 6 h) reversed the downregulation of ARF4 after P5091- or shRNA-mediated interference of USP7 (Fig. 5C, 5D). This implies that USP7 maintains the steady-state level of ARF4 through the proteasome pathway, which is consistent with our previous studies. Because USP7 is a deubiquitinating enzyme, we further hypothesized that USP7 regulates the stability of the ARF4 protein through deubiquitination. To test this hypothesis, we investigated whether blocking the function of USP7 would affect ARF4 ubiquitination. We used the Co-IP assay to assess the ubiquitination of ARF4.As shown in Fig. 5E and 5F, the ubiquitination activity of ARF4 was significantly increased after induction with P5091 or shRNA. This suggests that USP7 exerts a deubiquitinating effect on ARF4. Furthermore, we verified whether ARF4 ubiquitination triggered by blocking the function of USP7 is K48-ubiquitin related. We assessed the K48- and K63-ubiquitin levels of ARF4 with Co-IP. The results show that K48-ubiquitination of ARF4 increased after induction with P5091 or shRNA, whereas K63-ubiquitination did not change significantly (Fig. 5G, 5H). Together, these findings suggest that interference with USP7 decreases K48-deubiquitination of ARF4, thereby affecting the stability of ARF4.(Fig. 5I)

P5091 inhibits tumorigenicity in intracranial xenograft models

To investigate the therapeutic effect of P5091 on GBM, we established an intracranial orthotopic xenograft model by transplanting SHG-140 cells into the brain of small female nude mice. Starting from day 7 after successful implantation, PBS, 5 mg/kg of P5091 and 10 mg/kg of P5091 were injected intraperitoneally twice a week for 3 weeks. Subsequently, we observed tumor growth by bioluminescence imaging and hematoxylin eosin staining weekly, and used the tumor size and radiographic values as indicators to assess the treatment effect. We found that the growth rate of intracranial transplanted tumors in mice after the application of P5091 treatment was significantly lower than that of the blank control group (Fig. 6A, 6B). The survival time of mice treated with P5091 was significantly longer than that of mice in the blank control group (Fig. 6C). In addition, HE staining of brain sections from nude mice showed significant differences in tumor growth after treatment with P5091 (Fig. 6D). IHC staining analysis shows that the expression of apoptosis-related protein CLEAVED-CASPASE 3 was elevated, and the expression of BCL2 decreased, in the treated group, whereas the expression of USP7 did not differ significantly from that in the PBS group (Fig. 6E). The in vivo experiments yielded similar results to the in vitro experiments, in which P5091 inhibited the tumorigenicity of GBM and eventually caused an increase in the expression of apoptosis-associated proteins.

Discussion

GBMs are highly resistant to current therapeutic approaches.[27] Therefore, the discovery of other effective antitumor therapies may provide additional options for refractory GBM. In this study, we confirmed the role of USP7 as a new therapeutic target for GBM. The balance between ubiquitination and deubiquitination plays an important role in the homeostasis of the cellular protein pool.[28] In particular, the regulation of key proteins determines their tumorigenesis and progression. In the present study, we documented the therapeutic role of P5091, an inhibitor of the deubiquitinating enzyme USP7, in GBM. P5091 was originally identified as a specific inhibitor of USP7 by Chauhan et al. through a high-throughput screen. Using Ub-PLA2 enzyme reporter assays, the IC50 of P5091 against full-length USP7 was 4.2 mM.[29] P5091 acts as a covalent inhibitor of USP7, which covalently binds to the C223 residue of the catalytic domain of USP7, ultimately blocking its interaction with Ub to achieve anti-deubiquitination.[26] Although covalent inhibitors lack selectivity over non-covalent inhibitors, P5091 is not only highly specific but also irreversible.[30] In vitro, it is capable of inducing apoptosis and improving cellular drug resistance. P5091 can downregulate CCDC6 and increase PARP inhibitor sensitivity,[31] effectively prevent proliferation of ovarian cancer cells expressing wild-type P53, [25]or inhibit colorectal tumor growth by blocking the Wnt signaling pathway. [32]In our study, GBMs underwent significant concentration-dependent apoptosis through effective induction. This suggests that, as in other malignancies, P5091 can also induce GBM cell death. In in vivo experiments, among numerous small molecule inhibitors of USP7, P5091 was shown to be effective in treating tumors in vivo with little to no toxicity. [33, 34]Based on the fact that genetic deletion of USP7 in mice leads to early embryonic death between embryonic day 6.5 and 7.5, we believe that the application of P5091 is safer compared to knocking down USP7.[29] In our in vivo model, mice treated with the application of P5091 (5 mg/kg, 10 mg/kg) for 3 weeks on schedule showed no significant health problems. This is a preliminary indication of the potential of developing targeted drugs based on P5091, but more in vivo experimental data are still needed to analyze the efficacy and safety of P5091 for the treatment of GBM.

USP7 is a member of a family of deubiquitinating enzymes that contain more than 90 genes.[35] The deubiquitinase family of enzymes can deubiquitinate ubiquitin on specific substrates to prevent protein degradation by the proteasome or to regulate protein cellular functions. [36]Ubiquitins is conjugated to lysine residues in target proteins by ubiquitinating enzymes as mono- or poly-ubiquitin groups. Thus, they are involved in post-translational modifications that mediate protein stability and protein function.[8] However, the role of USP7 in cancer is paradoxical. For example, Li et al. showed that USP7 stabilizes the p53 protein and acts as a tumor suppressor through deubiquitination.[10] In contrast, the study by Cummins et al. found that another target substrate of USP7 is an E3 ligase, MDM2, and that MDM2 also has a regulatory effect on P53, which ultimately leads to the degradation of 53 and acts as an oncogene. [11]This suggests that USP7 can act as an oncogene or a tumor suppressor gene depending on the role played by its protein substrate and the amount of its own expression levels. In our study, we provide strong evidence for the identification of USP7 as an oncogene,especially in GBM. We tentatively reached this conclusion by observing apoptosis induced by the application of the suppression system of USP7.

Considering the diversity of USP7 substrates, we also analyzed the combined results of Co-IP and proteomics by mass spectrometry (MS) and screened possible substrates of USP7 in GBM. We

mechanistically elucidated the role of USP7 in stabilizing ARF4 through deubiquitination, thereby enhancing the anti-apoptotic capacity of GBM, which directly demonstrates that USP7 forms a complex with ARF4 in vitro. The significant reduction in the half-life of ARF4 observed after blocking the deubiquitination of USP7 and the detection of more ARF4 expression in vitro in cells after inhibition of proteasome activity suggests that USP7 regulates the stability of ARF4 by deubiquitination. Ub molecules contain seven lysine residues (Lys6, Lys11, Lys27, Lys29, Lys33, Lys48, and Lys63), different types and lengths of Ub chains can be formed, and that different types of Ub molecules connecting substrate proteins determine the fate of the tagged protein.[37] It is generally believed that proteins labeled by Lys-48-linked Ub chains regulate protein stability through proteasomal degradation, whereas proteins labeled by Lys-63-linked Ub chains perform nonproteolytic processes such as DNA repair and signal transduction.[38, 39]We hypothesized and verified the conjecture that USP7 mediates the stability of ARF4 by removing the Lys-48-linked Ub chain, but not the Lys-63-linked Ub chain.

In the current study, ARF4 was considered an anti-apoptotic factor. ARF4 inhibits BAX-induced apoptosis in yeast, and 4-HPR-induces apoptosis in mammalian cells and inhibited ROS production. This suggests that the anti-apoptotic effect of ARF4 may be related to the inhibition of ROS production. However, the molecular mechanism of ROS production inhibition by ARF4 and its role in apoptosis remain unclear.[20] In our study, we confirmed the anti-apoptotic effect of ARF4 on GBM cells. In addition, we found that overexpression of ARF4 in GBM cells rescued the apoptosis generated by P5091 or small interfering RNA-induced targeting of USP7. Our observations support a model(figure 5I), in which upregulation of USP7 in GBM leads to dysregulation of ARF4 protein modification, which enhances the anti-apoptotic capacity of GBM cells and ultimately leads to progress of the disease.

Conclusions

Inhibition of USP7 induces effective apoptosis of GBM cells in both in vivo and in vitro experiments, providing evidence for the development of P5091 as a new targeting therapeutic agent for GBM. These new findings regarding USP7 will provide a new strategy for the comprehensive treatment of GBM.

Declarations

Acknowledgements

None

Authors' contributions

YH and YZ contributed to the conception and design of the article, the analysis and interpretation of the data, and the critical revision of important elements of the article.TP and XL contributed to the design and analysis of the data, and drafted and revised the manuscript. ZT, HY, YW, GC and KZ contributed significantly to the conception and design, acquisition, analysis and interpretation of the data; and drafted and critically revised important intellectual elements of the article. All authors approved the final

version of the article and agreed to take responsibility for all aspects of the work and to ensure that issues relating to the accuracy or completeness of any part of the work were properly investigated and resolved. All authors have read and approved the final manuscript.

Funding

The National Science and Technology Resources Sharing Service Platform Program of China (Nos. YCZYPT[2020]06-1).

Availability of data and materials

The openly available data can be found in The Cancer Genome Atlas (TCGA) data portal (https://tcga-data.nci.nih.gov/tcga/) and Gene Expression Omnibus (GEO) database (GSE13507, https://www.ncbi.nlm.nih.gov/geo/query/acc.cgi?acc=GSE13507). We hereby undertake that all data and materials are available.

Ethics approval and consent to participate

All animal procedures and experimental methods were approved by the Ethics Committee of Soochow University and were conducted in accordance with the ARRIVE guidelines.

Consent for publication

All the authors agreed to be published.

Competing interests

There is no conflict of interest.

Author details

[1] Neurosurgery & Brain and Nerve Research Laboratory, The First Affiliated Hospital of Soochow University, Suzhou, Jiangsu, P. R. China.[2] Dushu Lake Hospital Affiliated to Soochow University, Suzhou, Jiangsu, P. R. China.

References

1. Louis DN, et al. The 2007 WHO classification of tumours of the central nervous system. Acta Neuropathol. 2007;114(2):97–109.
2. Stupp R, et al. Radiotherapy plus concomitant and adjuvant temozolomide for glioblastoma. N Engl J Med. 2005;352(10):987–96.
3. Aldape K, et al. Challenges to curing primary brain tumours. Nat Rev Clin Oncol. 2019;16(8):509–20.

4. Biau J, et al. Phase 1 trial of ralimetinib (LY2228820) with radiotherapy plus concomitant temozolomide in the treatment of newly diagnosed glioblastoma. Radiother Oncol. 2020;154:227–34.
5. Nininahazwe L, et al. The emerging nature of Ubiquitin-specific protease 7 (USP7): a new target in cancer therapy. Drug Discov Today; 2020.
6. Ristic G, Tsou WL, Todi SV. An optimal ubiquitin-proteasome pathway in the nervous system: the role of deubiquitinating enzymes. Front Mol Neurosci. 2014;7:72.
7. Maksoud S. The Role of the Ubiquitin Proteasome System in Glioma: Analysis Emphasizing the Main Molecular Players and Therapeutic Strategies Identified in Glioblastoma Multiforme. Mol Neurobiol; 2021.
8. Reyes-Turcu FE, Ventii KH, Wilkinson KD. Regulation and cellular roles of ubiquitin-specific deubiquitinating enzymes. Annu Rev Biochem. 2009;78:363–97.
9. Everett RD, et al. A novel ubiquitin-specific protease is dynamically associated with the PML nuclear domain and binds to a herpesvirus regulatory protein. EMBO J. 1997;16(7):1519–30.
10. Li M, et al. Deubiquitination of p53 by HAUSP is an important pathway for p53 stabilization. Nature. 2002;416(6881):648–53.
11. Cummins JM, et al., *Tumour suppression: disruption of HAUSP gene stabilizes p53.* Nature, 2004. **428**(6982): p. 1 p following 486.
12. Song MS, et al. The deubiquitinylation and localization of PTEN are regulated by a HAUSP-PML network. Nature. 2008;455(7214):813–7.
13. van der Horst A, et al. FOXO4 transcriptional activity is regulated by monoubiquitination and USP7/HAUSP. Nat Cell Biol. 2006;8(10):1064–73.
14. Cai JB, et al. Ubiquitin-specific protease 7 accelerates p14(ARF) degradation by deubiquitinating thyroid hormone receptor-interacting protein 12 and promotes hepatocellular carcinoma progression. Hepatology. 2015;61(5):1603–14.
15. Tavana O, et al. HAUSP deubiquitinates and stabilizes N-Myc in neuroblastoma. Nat Med. 2016;22(10):1180–6.
16. Moss J, Vaughan M. Structure and function of ARF proteins: activators of cholera toxin and critical components of intracellular vesicular transport processes. J Biol Chem. 1995;270(21):12327–30.
17. Shome K, Vasudevan C, Romero G. ARF proteins mediate insulin-dependent activation of phospholipase D. Curr Biol. 1997;7(6):387–96.
18. D'Souza-Schorey C, Chavrier P. ARF proteins: roles in membrane traffic and beyond. Nat Rev Mol Cell Biol. 2006;7(5):347–58.
19. Jang SY, Jang SW, Ko J. Regulation of ADP-ribosylation factor 4 expression by small leucine zipper protein and involvement in breast cancer cell migration. Cancer Lett. 2012;314(2):185–97.
20. Woo IS, et al. Identification of ADP-ribosylation factor 4 as a suppressor of N-(4-hydroxyphenyl)retinamide-induced cell death. Cancer Lett. 2009;276(1):53–60.

21. Cheng C, et al. Expression of HAUSP in gliomas correlates with disease progression and survival of patients. Oncol Rep. 2013;29(5):1730–6.
22. Li Y, et al. Characterization of a new human astrocytoma cell line SHG140: cell proliferation, cell phenotype, karyotype, STR markers and tumorigenicity analysis. J Cancer. 2021;12(2):371–8.
23. Fan YH, et al. USP7 inhibitor P22077 inhibits neuroblastoma growth via inducing p53-mediated apoptosis. Cell Death Dis. 2013;4(10):e867–7.
24. Xia X, et al. Deubiquitination and stabilization of estrogen receptor alpha by ubiquitin-specific protease 7 promotes breast tumorigenesis. Cancer Lett. 2019;465:118–28.
25. Wang M, et al. The USP7 Inhibitor P5091 Induces Cell Death in Ovarian Cancers with Different P53 Status. Cell Physiol Biochem. 2017;43(5):1755–66.
26. Zhang W, Sidhu SS. Drug development: Allosteric inhibitors hit USP7 hard. Nat Chem Biol. 2018;14(2):110–1.
27. Zhou D, et al. Distinctive epigenomes characterize glioma stem cells and their response to differentiation cues. Genome Biol. 2018;19(1):43.
28. Clague MJ, Heride C, Urbe S. The demographics of the ubiquitin system. Trends Cell Biol. 2015;25(7):417–26.
29. Chauhan D, et al. A small molecule inhibitor of ubiquitin-specific protease-7 induces apoptosis in multiple myeloma cells and overcomes bortezomib resistance. Cancer Cell. 2012;22(3):345–58.
30. Weinstock J, et al. Selective Dual Inhibitors of the Cancer-Related Deubiquitylating Proteases USP7 and USP47. ACS Med Chem Lett. 2012;3(10):789–92.
31. Malapelle U, et al. USP7 inhibitors, downregulating CCDC6, sensitize lung neuroendocrine cancer cells to PARP-inhibitor drugs. Lung Cancer. 2017;107:41–9.
32. An T, et al. USP7 inhibitor P5091 inhibits Wnt signaling and colorectal tumor growth. Biochem Pharmacol. 2017;131:29–39.
33. Zhang Y, et al. Conformational stabilization of ubiquitin yields potent and selective inhibitors of USP7. Nat Chem Biol. 2013;9(1):51–8.
34. Reverdy C, et al. Discovery of specific inhibitors of human USP7/HAUSP deubiquitinating enzyme. Chem Biol. 2012;19(4):467–77.
35. Clague MJ, et al. Deubiquitylases from genes to organism. Physiol Rev. 2013;93(3):1289–315.
36. Faesen AC, Luna-Vargas MP, Sixma TK. The role of UBL domains in ubiquitin-specific proteases. Biochem Soc Trans. 2012;40(3):539–45.
37. Ikeda F, Dikic I. Atypical ubiquitin chains: new molecular signals. 'Protein Modifications: Beyond the Usual Suspects' review series. EMBO Rep. 2008;9(6):536–42.
38. Hershko A, Ciechanover A. The ubiquitin system. Annu Rev Biochem. 1998;67:425–79.
39. Komander D, Rape M. The ubiquitin code. Annu Rev Biochem. 2012;81:203–29.

Figures

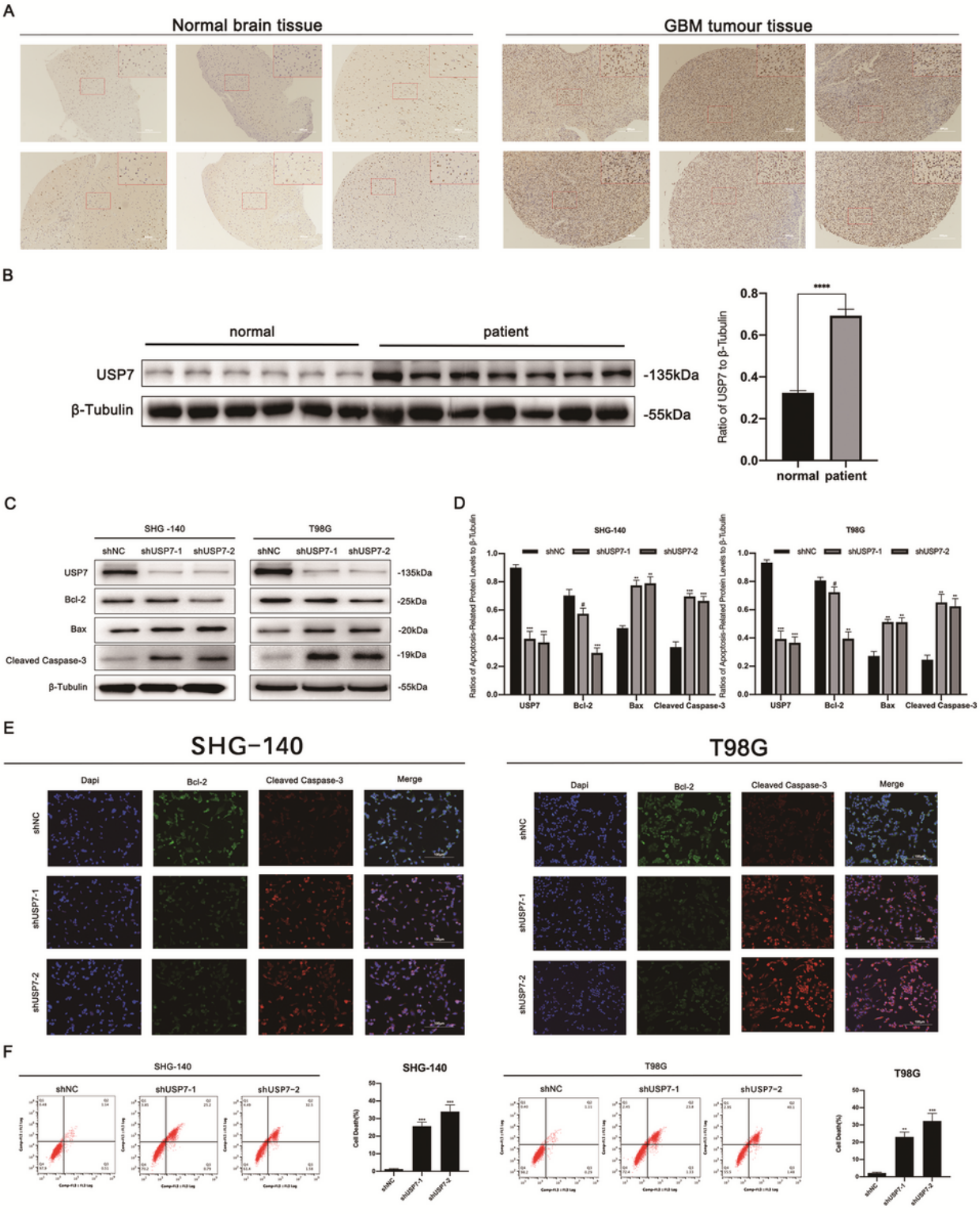

Figure 1

USP7 is highly expressed in GBM cells and its inhibition induces apoptosis. A. Immunohistochemical staining of USP7 in human glioblastoma and normal brain tissue samples. Scale bar, 300 μm. B. Western blotting analysis of USP7 protein levels in primary glioblastoma tissue samples and normal brain tissue samples, n>6. C&D. SHG-140 and T98G cells were treated with two different shUSP7s for 24 h. The changes in apoptotic proteins were observed by Western blotting analysis, n=3. E. Immunofluorescence

analysis of SHG-140 and T98G, cells were stained with DAPI and antibodies against BCL-2 or CLEAVED-CASPASE-3. Scale bar, 100 μm. F. Apoptosis rate of SHG-140 and T98G cells treated by shUSP7s was measured by flow cytometry, n=3.All statistics are expressed as mean±S.E.M., #P=NS, *P<0.05,**P<0.01, ***P<0.001 or ****P<0.0001, Student's t-test.

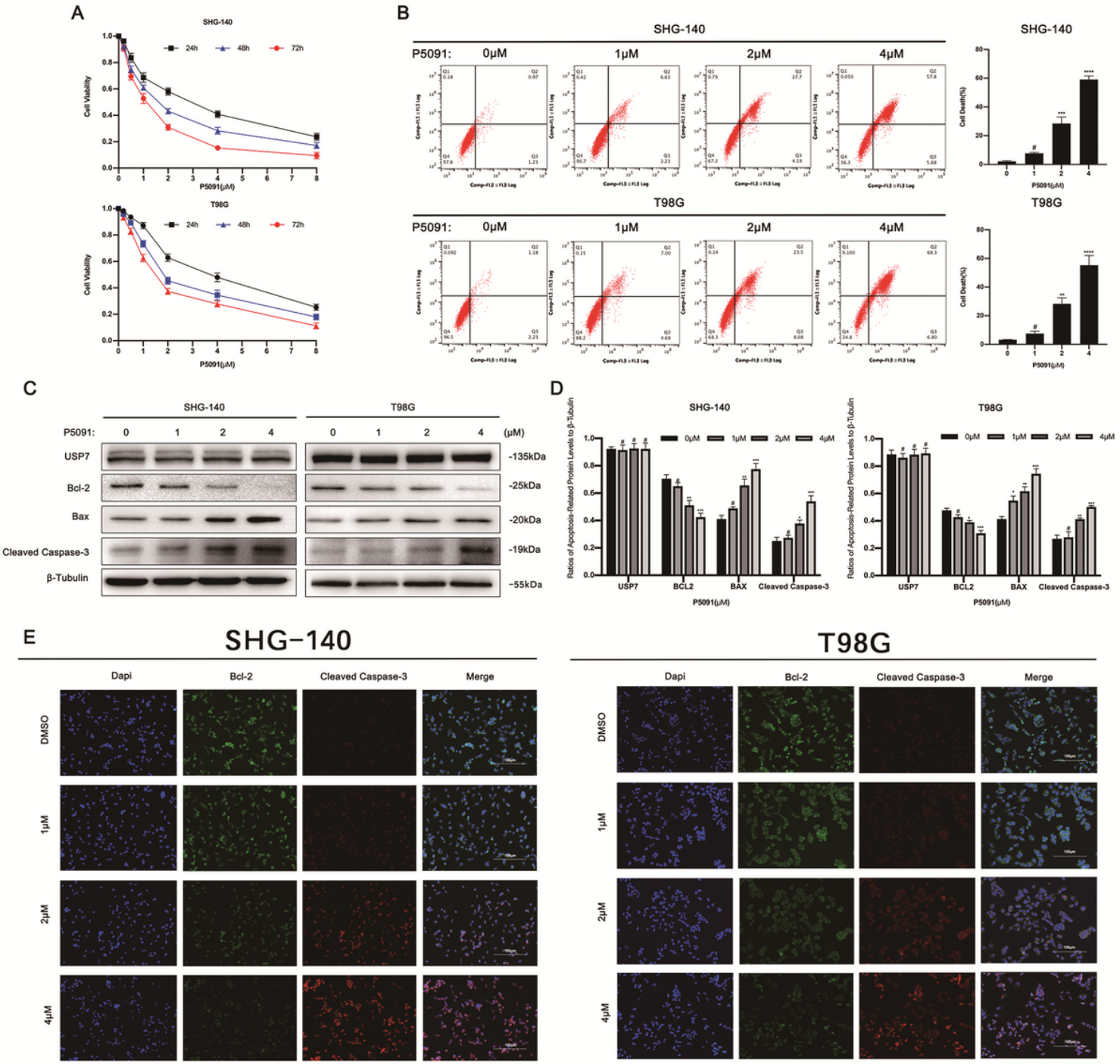

Figure 2

P5091 induces apoptosis in GBM cells. A. SHG-140 and T98G cells were treated with P5091 for 24, 48, and 72 h. Cell viability was determined by CCK-8 assay. B. The apoptotic rate of SHG-140 and T98G cells

treated with different concentrations of P5091 for 48 h was measured by flow cytometry, n=3. C&D. SHG-140 and T98G cells were treated with P5091 for 48 h. Changes in apoptotic proteins were observed by Western blotting analysis, n=3. E. Immunofluorescence analysis of SHG-140 and T98G, cells were stained with DAPI and antibodies against BCL-2 or CLEAVED-CASPASE 3. Scale bar, 100 μm. All statistics are expressed as mean±S.E.M., #P=NS, *P<0.05,**P<0.01, ***P<0.001 or ****P<0.0001, Student's t test.

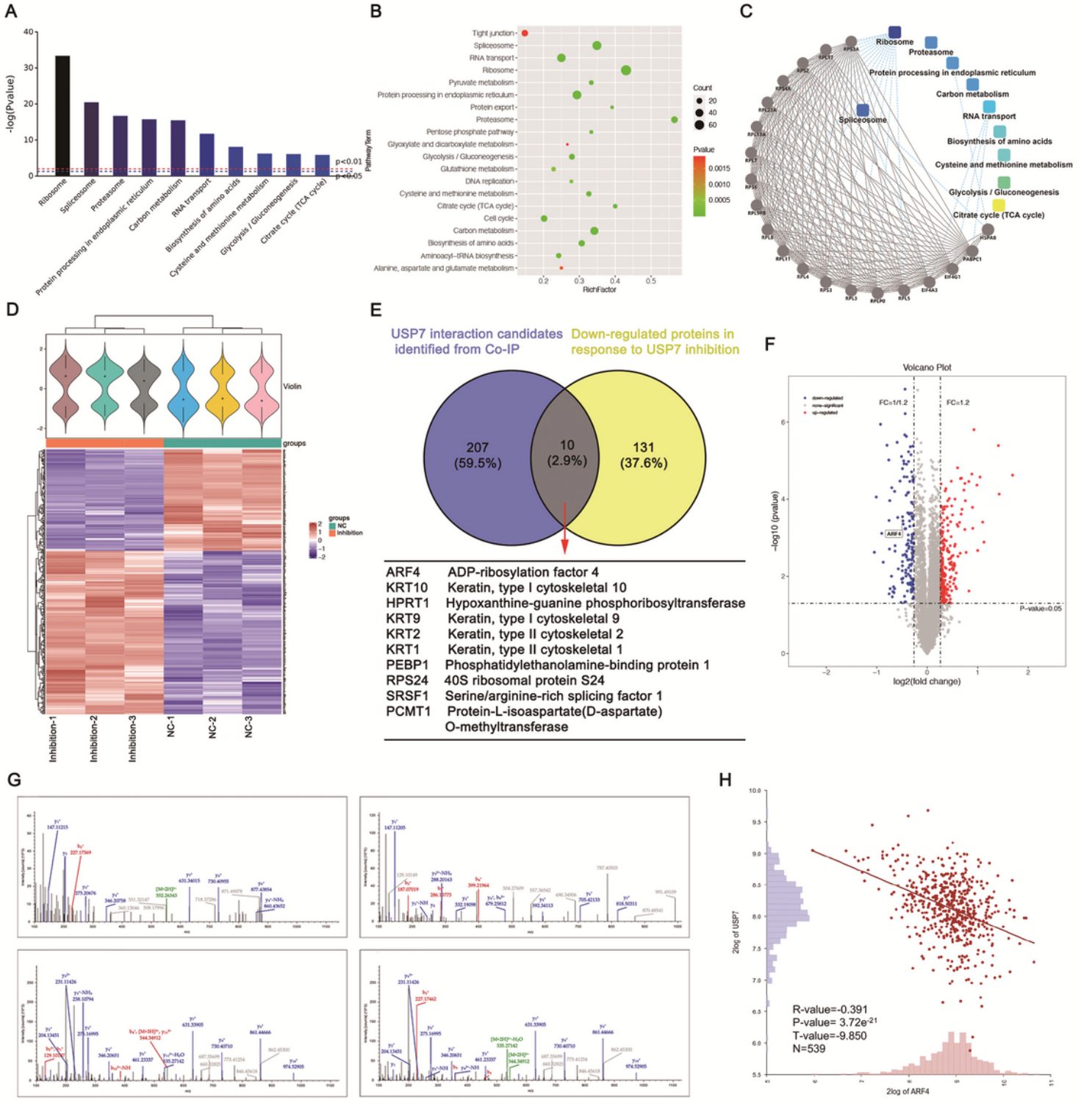

Figure 3

ARF4 binds to USP7 and is downregulated by USP7 inhibition. A-C. Proteins bound to USP7 were identified in SHG-140 by Co-IP and MS, and the screened proteins were analyzed for the KEGG pathway. D. Heat map showing the comparative results of TMT proteomics analysis after 48 h treatment using DMSO or P5091 (2μM) in SHG-140. E. Venn diagram showing down-regulated proteins in response to P5091 (yellow), USP7 interaction candidates identified by Co-IP (purple), and overlapping proteins. F. Volcano plot showing the differential proteins from TMT proteomics analysis and the location of ARF4. G. Secondary mass spectra of the four peptides of ARF4. H. Expression correlation analysis of USP7 with ARF4 in the TCGA database.

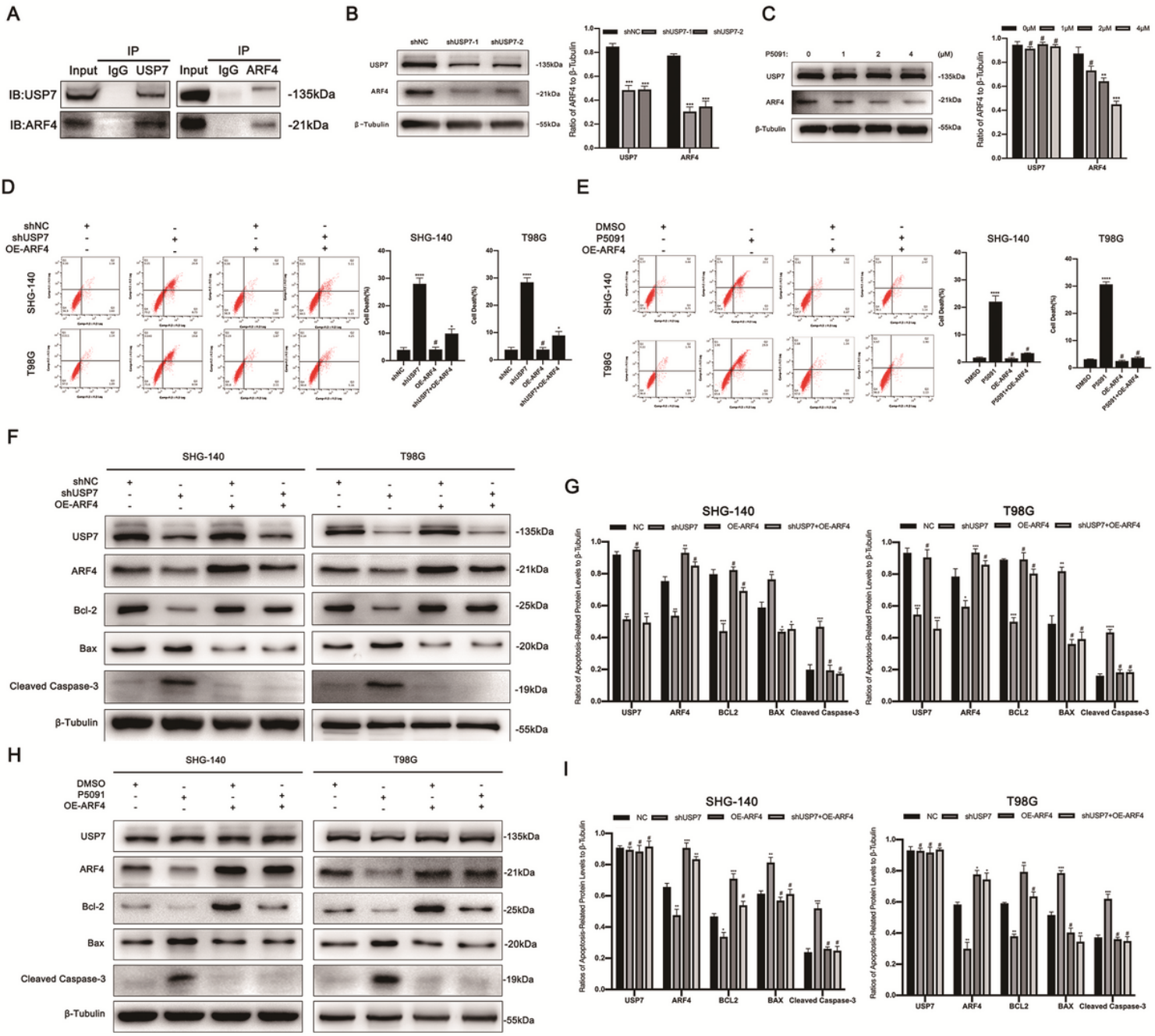

Figure 4

Overexpression of ARF4 rescues apoptosis resulting from USP7 interference A. Interaction between USP7 and ARF4 in SHG-140 was determined using the Co-IP assay. B. SHG-140 cells were transfected with different shUSP7 for 24 h and ARF4 expression was determined by western blotting, n=3. C. Expression of ARF4 was determined by western blotting after treatment of SHG-140 with different concentrations of P5091 for 48 h,n=3. D&E. Changes in apoptotic rate after overexpression of ARF4 in SHG-140 and T98G cells treated with P5091 (2 μM) for 48 h or transfected with shUSP7 for 24 h were detected by flow cytometry,n=3. F-I. Changes in apoptotic proteins after overexpression of ARF4 in SHG-140 and T98G cells treated with P5091 (2 μM) for 48 h or transfected with shUSP7 for 24 h were observed by Western blotting analysis, n=3. All statistics are expressed as mean±S.E.M., #P =NS, *P<0.05 ,**P<0.01 or ***P<0.001, Student's t test.

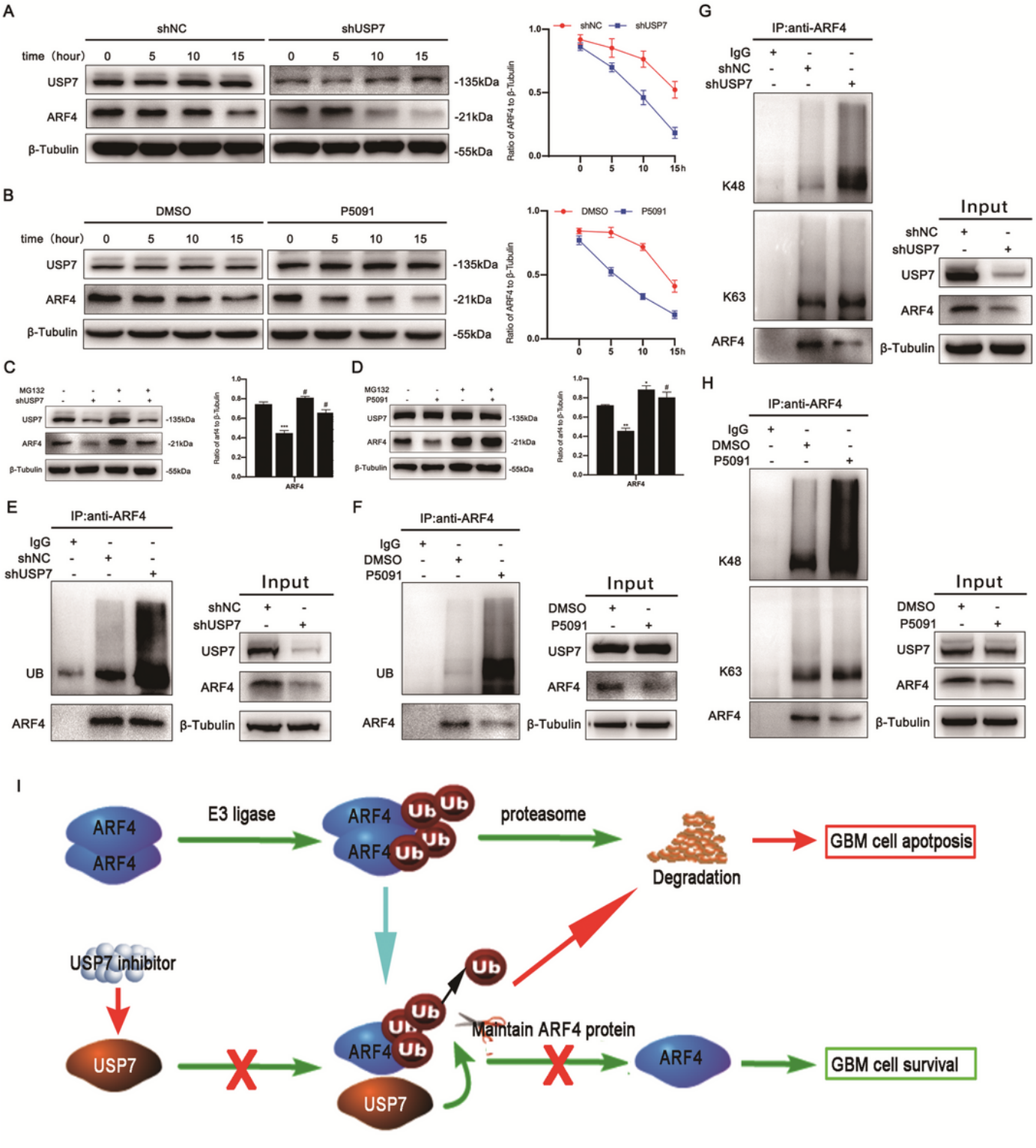

Figure 5

USP7 regulates ARF4 stability through K48-linked deubiquitination A&B. After transfection of SHG-140 cells with shUSP7 for 24 h or treatment of cells with P5091 (2 μM) for 48 h, cells were treated with CHX (100 μg/ml) at different times and ARF4 expression was analyzed by Western blotting, n=3. C&D. SHG-140 cells were transfected with shUSP7 for 24 h or treated with P5091 (2 μM) for 48 h followed by treatment with the proteasome inhibitor MG132 (10 μM) for 6 h. ARF4 expression was analyzed by

Western blotting, n=3. E&F. SHG-140 cells were transfected with shUSP7 for 24 h or treated with P5091 (2 μM) for 48 h followed by treatment with MG132 (10 μM) for 6 h. The protein extracts were immunoprecipitated with IgG beads of anti-ARF4, and then ubiquitin and ARF4 expression were detected by western blotting. G&H. SHG-140 cells were transfected with shUSP7 for 24 h or treated with P5091 (2 μM) for 48 h followed by treatment with MG132 (10 μM) for 6 h. The protein extracts were immunoprecipitated with IgG beads of anti-ARF4, and then the expression of K48-ubiquitin, K63-ubiquitin and ARF4 was detected by western blotting. I. A proposed mechanism for USP7 to regulate the ARF4 level in GBM. All statistics are expressed as mean±S.E.M., #P=NS, *P<0.05,**P<0.01 or ***P<0.001, Student's t test.

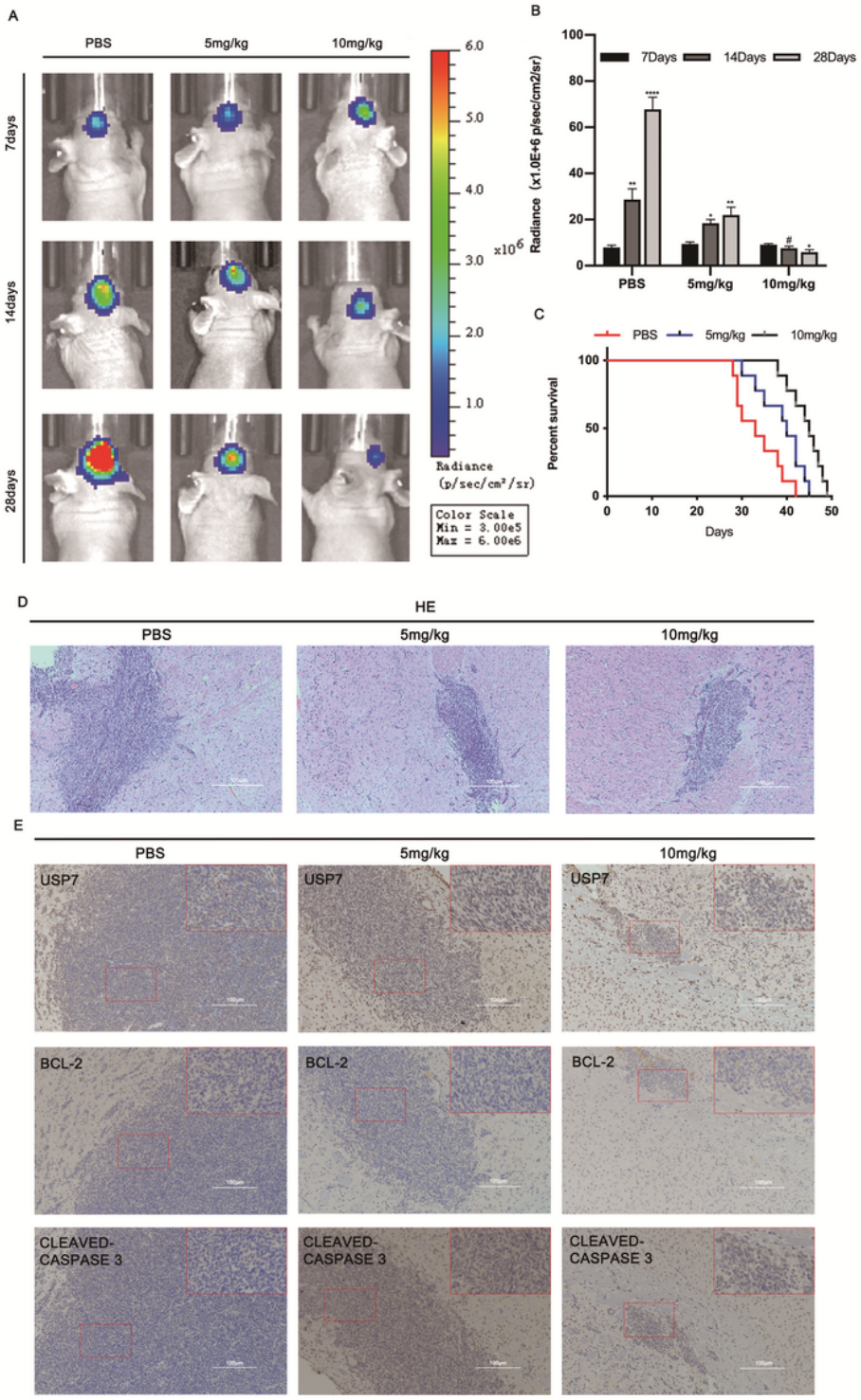

Figure 6

P5091 inhibits tumorigenicity in intracranial xenograft models Female BALB/c nude mice were injected intraperitoneally with PBS, P5091 (5 mg/kg/day, 10 mg/kg/day) and treated 2 days per week. Treatment started on day 7 after implantation and lasted for approximately 21 days. A. Representative images of bioluminescence in mice on days 7, 14 and 28 after implantation. B. Quantitative analysis of these bioluminescence images, n=6. C. Overall survival of the PBS and P5091 treatment groups, n=6. D.

Representative HE images of tumor sections. Scale bar, 100 μm. E. Representative IHC images of tumor sections for anti-USP7, anti-BCL-2 and anti-CLEAVED-CASPASE. Scale bar, 100 μm. All statistics are expressed as mean±S.E.M., #P=NS, *P<0.05,**P<0.01 or ****P<0.0001, Student's t test.